Applied Thermal Engineering 41 (2012) 52–60

Contents lists available at SciVerse ScienceDirect

Applied Thermal Engineering

journal homepage: www.elsevier.com/locate/apthermeng

Thermal design of a tray-type distillation column of an ammonia/water absorption refrigeration cycle

E.W. Zavaleta-Aguilar, J.R. Simões-Moreira*

SISEA – Alternative Energy Systems Laboratory in the Mechl. Eng. Department at Escola Politécnica, Post-Graduation Program on Energy of Institute of Electrotechnical and Energy, University of São Paulo, Brazil

ARTICLE INFO

Article history:
Received 10 April 2011
Accepted 5 December 2011
Available online 11 December 2011

Keywords:
Distillation column
Ammonia/water
Refrigeration
Absorption

ABSTRACT

The goal of this paper is to present an analysis of a segmented weir sieve-tray distillation column for a 17.58 kW (5 TR) ammonia/water absorption refrigeration cycle. Balances of mass and energy were performed based on the method of Ponchon-Savarit, from which it was possible to determine the ideal number of trays. The analysis showed that four ideal trays were adequate for that small absorption refrigeration system having the feeding system to the column right above the second tray. It was carried out a sensitivity analysis of the main parameters. Vapor and liquid pressure drop constraint along with ammonia and water mass flow ratios defined the internal geometrical sizes of the column, such as the column diameter and height, as well as other designing parameters. Due to the lack of specific correlations, the present work was based on practical correlations used in the petrochemical and beverage production industries. The analysis also permitted to obtain the recommended values of tray spacing in order to have a compact column. The geometry of the tray turns out to be sensitive to the charge of vapor and, to a lesser extent, to the load of the liquid, being insensible to the diameter of tray holes. It was found a column efficiency of 50%. Finally, the paper presents some recommendations in order to have an optimal geometry for a compact size distillation column.

1. Introduction

Worldwide population increase is directly accompanied by an electrical and basically all other forms of energy demand boost. Air conditioning, refrigeration, and heating systems are accountable for a considerable fraction of the electrical energy matrix in many countries. The increase in energy consumption and the scenario of energy shortage in near future have brought back the concept of a rational and efficient use of energy and its transformations into useful mechanical, electrical, and thermal energy. In this context, absorption refrigeration cycles are a key component in both refrigeration and air conditioning systems that can be powered by waste thermal energy at basically very little operational costs and electricity consumption. Thermal energy sources needed for powering those cycles can be supplied by waste heat from thermal processes, by solar energy, by exhaust gases from engines and turbines, and by basically any other available heat source above its operational temperature. Therefore, if one includes an absorption refrigeration cycle in a cogeneration or trigeneration system, i.e., the simultaneous generation of electricity, heat and cold from a single source of energy, this concept of an integrated power plant becomes a more efficient, economical and environmentally more friendly. The most common working fluids in absorption refrigeration cycles are the pairs of fluids ammonia/water and lithium bromide/water, being the former natural fluids. An ammonia/water absorption refrigeration cycle (*AARC*) achieves subzero cooling temperatures, since the refrigerant is ammonia, while the lithium bromide/water technology is bound by the lower theoretical temperature of 0.01 °C, because water is the working fluid refrigerant. This work deals with ammonia/water mixtures.

A critical element of any *AARC* is the distillation column in which a simultaneous heat and mass transfer process takes place in the two-phase, two-component mixture of ammonia/water. The distillation column must provide ammonia vapor at a high grade of purity. Otherwise, if the ammonia vapor is too wet, the water content can continuously be accumulated in the evaporator causing a degradation of the cycle *COP* (coefficient of performance) [1,2]. Ahachad et al. [3] compared the *COP* of a simple effect *AARC* operating with and without a purification system. In place of the rectifier they tested a vapor bubble purifying system. The *COP* of the absorption chiller with vapor bubble purifying system improved from 15 % to 35 % and the required area of solar collectors, used as a heat source, was lowered by 10%; their highest *COP* obtained was 0.4.

* Corresponding author. Escola Politécnica da USP/PME, Av. Prof. Mello Moraes, 2231, 05508-900, São Paulo, SP, Brazil. Tel./fax: +55 11 30915684.
E-mail address: jrsimoes@usp.br (J.R. Simões-Moreira).

1359-4311/$ – see front matter © 2011 Elsevier Ltd. All rights reserved.
doi:10.1016/j.applthermaleng.2011.12.009

Nomenclature

AARC	ammonia/water absorption refrigeration cycle
COP	coefficient of performance [−]
CV	control volume
D	column diameter [m]
d	tray hole diameter [m]
f	factor [-]
h	specific enthalpy [kJ/kg]
L	length [m]
m	mass flow rate [kg/s]
N	number of trays
NOM	nominal
P	pressure [Pa]
Q	heat load [kW]
R	reflux ratio [-]
x	mass fraction [-]

Greek

Δ	variation [−]
η	efficiency [−]

Subscripts

a	actual
c	column
d	distilled
enr	enriching
E	evaporator
f	feed
G	generator
i	ideal
L	liquid
min	minimum
n, m	a generic tray number
r	reflux
R	rectifier, residual
str	stripping
t	tray
ts	tray spacing
V	vapor
w	waste, weir

Other problem with a high degree of water vapor in ammonia vapor is the increase of the vaporization temperature associated with such binary solutions during a phase change, a process known as *temperature glide*. If the vaporization temperature keeps rising, the system will reach a point where it will no longer be possible to cool down the medium of interest by the evaporator. This temperature behavior avoids the use an ammonia/water mixture at substantial concentrations of water vapor [1,4]. The higher the concentration of water vapor, the more significant will the temperature glide be. Therefore, it is crucial to remove water vapor in excess from the ammonia vapor that exits the generator to ensure the reliability and efficiency of ammonia/water absorption refrigeration systems [5]. It has been suggested that a purity grade of approximately 99.9% wt of ammonia as the least concentration for a proper *AARC* operation [6].

Herold et al. [4] and Kuehn [7] presented a conceptual design analysis of distillation columns of an *AARC* without any in-depth study of working parameters such as reflux, strong solution feeding position as well as heat fluxes involved in the generator and the rectifier. Anand and Erickson [8] analyzed a tray distillation column of a 28.1 kW (8 TR) *AARC* emphasizing designing parameters such as flooding prevention, tray holes weeping and column geometry. Sieres et al [9]. carried out experimental studies of purification systems for an *AARC* with random and structured assembling of commercial packing types. Their tests showed that the pall packing type performed better than other packing tested and it also required a lower packing height for a desired ammonia vapor grade of purity. Mendes [10] found that lower heights for the same purification grade was found for a column filled with the novalox type packing than that for a plain spray column type. However, no experimental results were found in the literature about using tray distillation column in *AARC*.

This paper studies the distillation process of the ammonia/water solution to obtain a high grade of purity ammonia vapor. The analysis provides geometrical details to achieve pre-established purity values. This study chose a sieve-tray column, since its design is simple, besides being economical, having a plain cleaning maintenance, low pressure drop, and it is suitable for most applications. Multiple entrances and exits are more flexible in tray columns when compared with the packing column ones.

Studies available in open literature about gas-liquid direct contact trays are based on two methods for carrying out a mass and energy balance: the Ponchon-Savarit method and the McCabe-Thiele's. Bogart [5] and Treybal [11] showed that the former method is more accurate, since the other one considers constant liquid and vapor flow rates. By using the Ponchon-Savarit method the conservation and constitutive equations were solved using commercial software (EES — *Engineering Equation Solver*) to solve the non-linear system of coupled equations and for thermodynamic and transport properties calculation.

2. Distillation column description

Schematic of an *AARC* is shown in Fig. 1a, where it can be observed the distillation column in bold line. The distillation column is made up of other parts as illustrated in more details on the expanded view in Fig. 1b. There exists a reservoir of ammonia/water liquid solution inside the distillation column (Fig. 1b) which is called "the generator". In the generator the ammonia/water solution is brought in contact with heated surfaces and, consequently, part of the solution will vaporize given rise to a vapor phase rich in ammonia, given that it is the most volatile component.

Wet ammonia vapor rises up the column in a counter flow direction to the descending liquid solution (Fig. 1b). As the vapor rises up inside the column through the many trays its purity grade keeps increasing, i.e., higher concentration of ammonia is achieved each time, while the ammonia concentration in descending solution diminishes. When the ammonia vapor reaches the top tray (numbered 1 in Fig. 1b) still containing some water vapor, it passes through a partial condenser called "the rectifier", where heat is removed and part of the water vapor is condensed along with some amount of ammonia due to thermodynamic equilibrium conditions. The liquid and vapor are directed to the accumulator where they are separated: the condensed liquid is driven back to the top of the column (reflux) and the high purity ammonia vapor exits the piece of equipment in direction to the main condenser.

3. Thermodynamic modeling

Fig. 1b also shows the variables involved in the mass and energy balance in the distillation column used in the Ponchon-Savarit

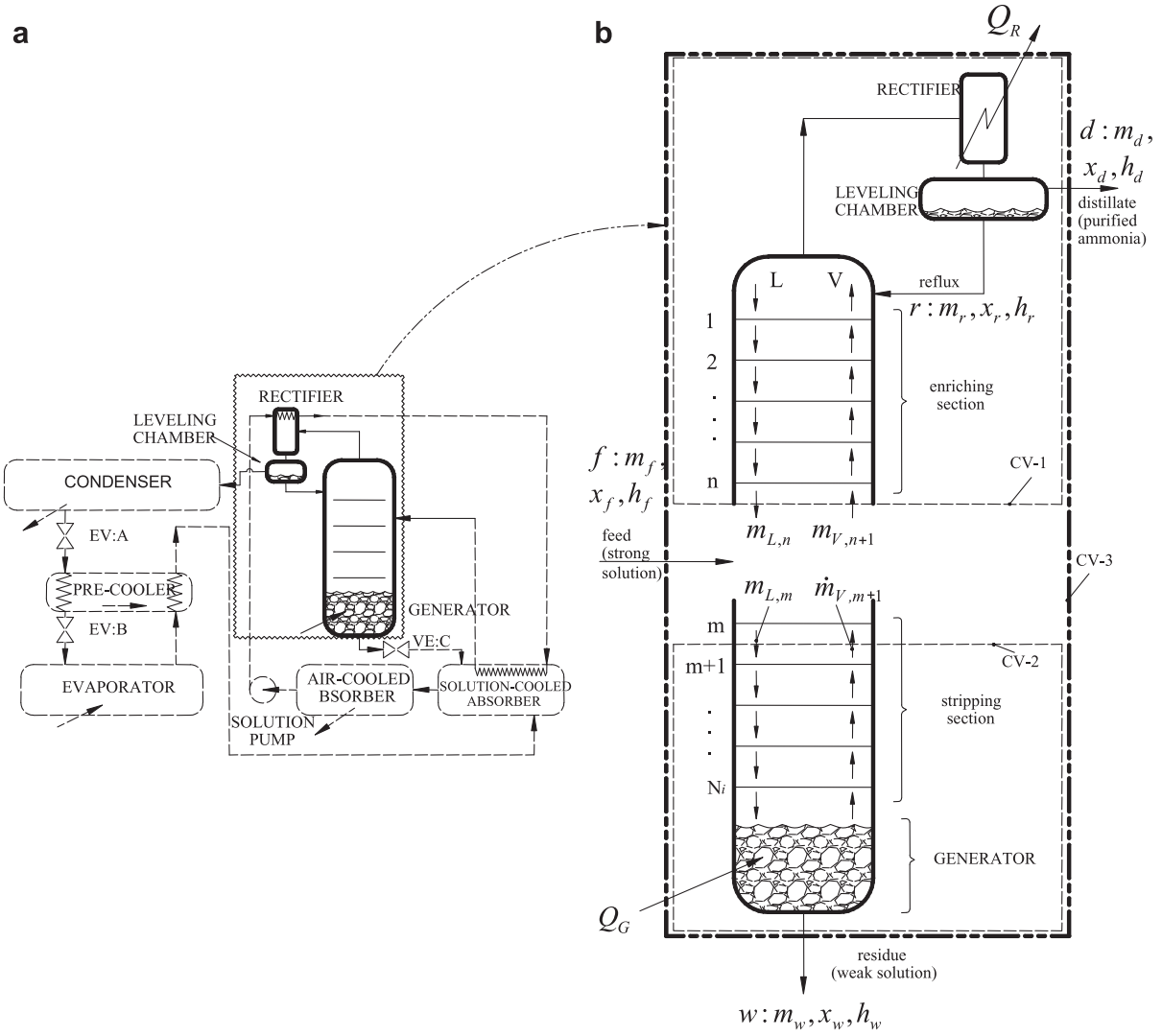

Fig. 1. (a) Distillation column (in bold line) as part of an *AARC*; (b) Expanded view of the distillation column and relevant variables for the mass and energy balance analyses.

method analysis described further on. It is convenient to define three control volumes (*CVs*) in order to carry out a detailed analysis of each section in the column. The overall control volume *CV-3* includes the column strong solution feeding system and the label *"f"* is assigned to it; the weak solution exit is labeled *"w"*, and the exiting purified ammonia vapor is labeled *"d"*. According to Kuehn et al. [7] the enriching and stripping sections are named "the analyzer". In Fig. 1b, "*L*" and "*V*" are the liquid solution and vapor phase, respectively; "*r*" stands for the "reflux". In the column there are N_i ideal trays, having n trays in the enriching section and $N_i - m + 1$ trays in the stripping section. Considering the control volume *CV-1* seen in Fig. 1b, the mass and energy balance yields to:

$$\frac{m_{L,n}}{m_{V,n+1}} = \frac{x_d - x_{V,n+1}}{x_d - x_{L,n}} = \frac{h'_d - h_{V,n+1}}{h'_d - h_{L,n}} \tag{1}$$

where, the specific enthalpy h'_d is given by:

$$h'_d = h_d + \frac{Q_R}{m_d} \tag{2}$$

The relationship between the mass fraction of ammonia and specific enthalpy in Eq. (1) represents an operation line. The balances of mass and energy from tray 1 to tray n provide the operation line in the $h - x$ diagram, and they all coincide at the point (x_d, h'_d). The liquid and vapor leaving each tray are at thermodynamic equilibrium ($m_{L,n}$, $m_{V,n}$) and they are linked by the "tie lines" in the $h - x$ diagram. The projection of the mass fractions ($x_{L,n}$, $x_{V,n+1}$) corresponding to the operating line in the $h - x$ diagram onto the $x_V - x_L$ diagram provides a point that belongs to the operation curve. The projections of all mass fractions of the operating lines provide the operation curve corresponding to the side of enriching. Those projections in the $x_V - x_L$ diagram create triangle shapes, each triangle is one ideal tray of the enriching section.

It is defined the reflux ratio "*R*" (or external reflux ratio) as the ratio between the mass flow rate of saturated liquid that returns from the leveling chamber in Fig. 1b to the top of the enriching section and the mass flow rate of saturated vapor leaving the column (d). From the mass and energy balance of the first tray, the rectifier and the distillate vapor is obtained:

$$R = \frac{m_r}{m_d} = \frac{h'_d - h_{V,1}}{h_{V,1} - h_r} \tag{3}$$

From the mass and energy balance for the control volume *CV-2* in Fig. 1b, it yields to:

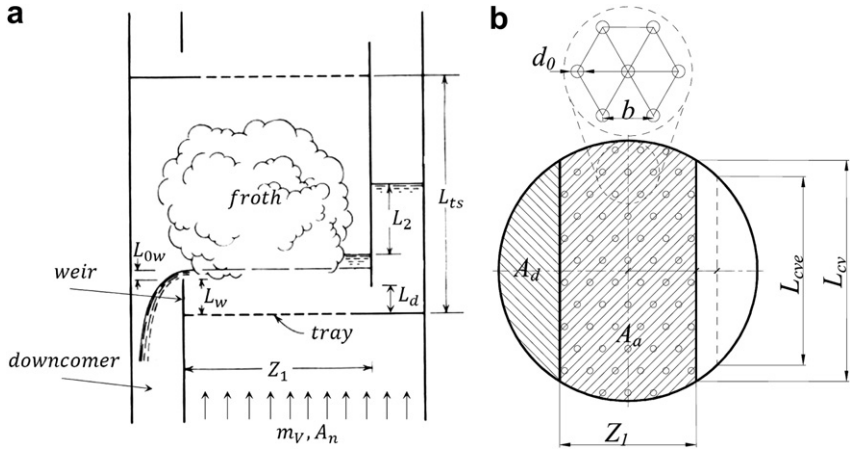

Fig. 2. Tray geometry (left, adapted from Treybal, 1981).

$$\frac{m_{L,m}}{m_{V,m+1}} = \frac{x_{V,m+1} - x_w}{x_{L,m} - x_w} = \frac{h_{V,m+1} - h'_w}{h_{L,m} - h'_w} \tag{4}$$

where, the specific enthalpy h'_w is given by:

$$h'_w = h_w - \frac{Q_G}{m_w} \tag{5}$$

As seen in the previous analysis, the relationship between specific enthalpy and mass fractions in Eq. (4) provides operating lines that coincide at the point (x_w, h'_w). The projections of points corresponding to the saturated mass fractions of the operation lines of $h - x$ diagram onto $x_V - x_L$ diagram provide points of the operational curve. If these points are connected together it is obtained the stripping operation curve. Those projections in the $x_V - x_L$ diagram create triangle shapes, each triangle is one ideal tray of the stripping section. The strong solution feeding to the column should be on the tray corresponding to the intersection of the enriching and stripping operation curves. If the feed point is above or below of this point, it would necessary more trays to obtain the desired concentration x_d and x_w, at distillated vapor exit and weak solution exit respectively. Joining together the stripping section-generator with the enriching section-rectifier, it is obtained the complete distillation column. Making the overall mass and energy balance of the distillation column for the control volume *CV-3* enveloping all pieces of equipment in Fig. 1b one will obtain:

$$\frac{m_d}{m_w} = \frac{x_f - x_w}{x_d - x_f} = \frac{h_f - h'_w}{h'_d - h_f} \tag{6}$$

The relationship between the ammonia mass fraction and the specific enthalpy in Eq. (6) gives the overall operating line in the $h - x$ diagram. If the overall operating line coincides with an equilibrium line then it is obtained the "minimum reflux ratio" ($R_{\min}$) condition, under these situations the number of trays required for the concentration of ammonia vapor desired is very large and the heat flows necessary to be supplied to the generator and removed from rectifier are minimum. When all the vapor flow leaving the top tray of the enriching section is condensed and returns back to the column, and the feeding to the column and the weak solution exit are halted, the distillation system arrives to the "total reflux" condition, under these situation the number of trays necessaries at the columns is minimum and the heat fluxes involved in the generator and rectifier are very large. Kister [12] indicates that it should be used a reflux factor (Eq. (7)), f_R between 1.05 and 1.3, whose definition is given by:

$$f_R = \frac{R}{R_{\min}} \tag{7}$$

where R is the actual reflux ratio and $R_{\min}$ the minimum one. $R_{\min}$ depends on the equilibrium thermodynamic characteristic of the distillated substances and the feeding, distillation, and residue conditions (see Fig. 1b).

4. Hydraulic and internal geometry distillation column considerations

It is shown in Fig. 2a and b the geometry of the segmented weir sieve-tray with indication of dimensional designing parameters and magnitudes.

Tray holes allow vapor to pass through a tray while the downcomer allows the admission of liquid to the tray. There are flow regimes of liquid and vapor suitable for the distillation column to perform properly [12,13]. Outside these regimes there exist mixture inefficiencies at the tray such as "flooded column" that appears when the liquid or vapor flows are high. On the other hand, when the vapor flow is very small, liquid weeping through the holes of the tray happens.

For designing purposes it is also relevant to consider the vapor pressure drop across each tray. According to reference [11] the vapor pressure drop, ΔP_v is influenced by three pressure drops as the flow goes through each tray. The first one is defined when the vapor crosses a dry tray (ΔP_t); the second one when passing through the liquid (ΔP_L); and last one, called residual pressure drop (ΔP_R), when the vapor overcomes the surface tension. There is also a liquid pressure drop (ΔP_d) when it flows through downcomer. A detailed study of the internal geometry and the pressure drops was carried out by Zavaleta-Aguilar [14] and his study results are employed throughout this work.

5. Distillation column efficiency

Ideal trays consider the mixing time between liquid and vapor entering the tray is long enough for them to leave the tray at a thermodynamic equilibrium condition, but in actual operation these ideal equilibrium conditions do not take place. Thus, the actual analysis of liquid and vapor phases mixture should consider the transport phenomena between those phases and their forming components. For this reason, an efficiency method is frequently used by many authors [12,15,16]. The method considers that the

Table 1
Input variables for mass and energy balance in the distillation column.

Position	Mass flow (kg/s)	Mass fraction (–)	Temperature (°C)
d	0.015	0.999	–
f	–	0.452	98.14
w	–	0.152	–

actual number of trays is fixed by the efficiency of the column, according to Eq. (8):

$$N_a = \frac{N_i}{\eta_c} \tag{8}$$

where N_a represents the actual number trays of the column, N_i the ideal number of trays (calculated by the Ponchon-Savarit method) η_c and efficiency of the column. This efficiency can be evaluated analytically considering the efficiency of point (η_{PV}), the Murphree efficiency (η_{MV}), and the Murphree efficiency corrected by entrainment efficiency (η_{MVE}). Finally the column efficiency is related to η_{MVE} by the Lewis equation. Additional information on these efficiencies can be found in references [12,15,16].

6. Results and discussions

For a 17.58 kW (5 TR) *AARC* operating at a −2 °C evaporation temperature and at a 40 °C condensation temperature with an ammonia vapor concentration set at 99.9% wt, the main cycle operation values are shown in Table 1. They were obtained from a thermodynamic analysis [17]. Those data were used as input values for designing the distillation column in this work. For these conditions the pressure inside the distillation column is 1556 kPa.

In Table 1 the first column indicates the flow position location as given in Fig. 1b. Only the purified ammonia mass flow rate (label "*d*") was needed for the calculations as shown in the second column. Strong solution temperature was 98.14 °C. Purified saturated ammonia vapor leaves the column at the top and weak solution, also saturated, leaves the column at the bottom. The third column shows the mass fraction at the indicated positions obtained from the thermodynamic modeling. The reflux factor, f_R, is assumed to be 1.1, this factor will be analyzed later on in a sensitive analysis study. With those input variables provided, an *EES* program to solve Eqs. (1)–(7) was developed. The output data are useful for obtaining several designing parameters as shown graphically in Figs. 3 and 4 that are discussed next.

Fig. 3a and b show the strong solution feeding position "*f*", the weak solution exiting point "*w*" (weak solution), and "*d*", the distillate ammonia vapor leaving the distillation column. In the *h*–*x* diagram in Fig. 3a is also shown the equilibrium lines, operation lines. and the overall operation line. It is shown in Fig. 3b a schematic of the distillation column, where it can be seen the location of the strong solution entry "*f*" in the column just above the tray 2. The ideal number of trays, N_i, for achieving 99.9% wt purification grade

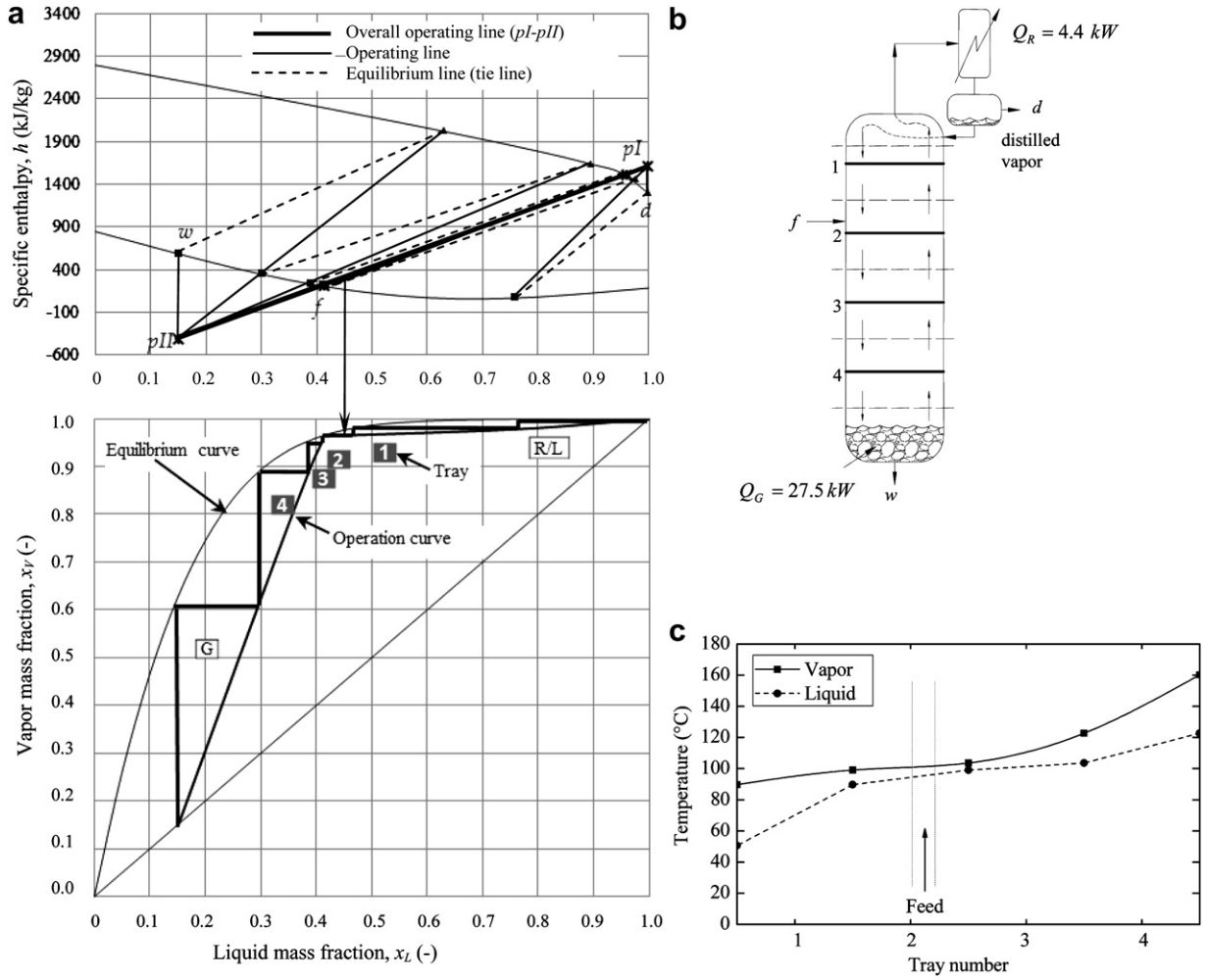

Fig. 3. (a) $h - x$ and $x_V - x_L$ diagrams for the distillation process; (b) distillation column diagram; (c) Vapor and liquid flow temperature variation in the distillation column.

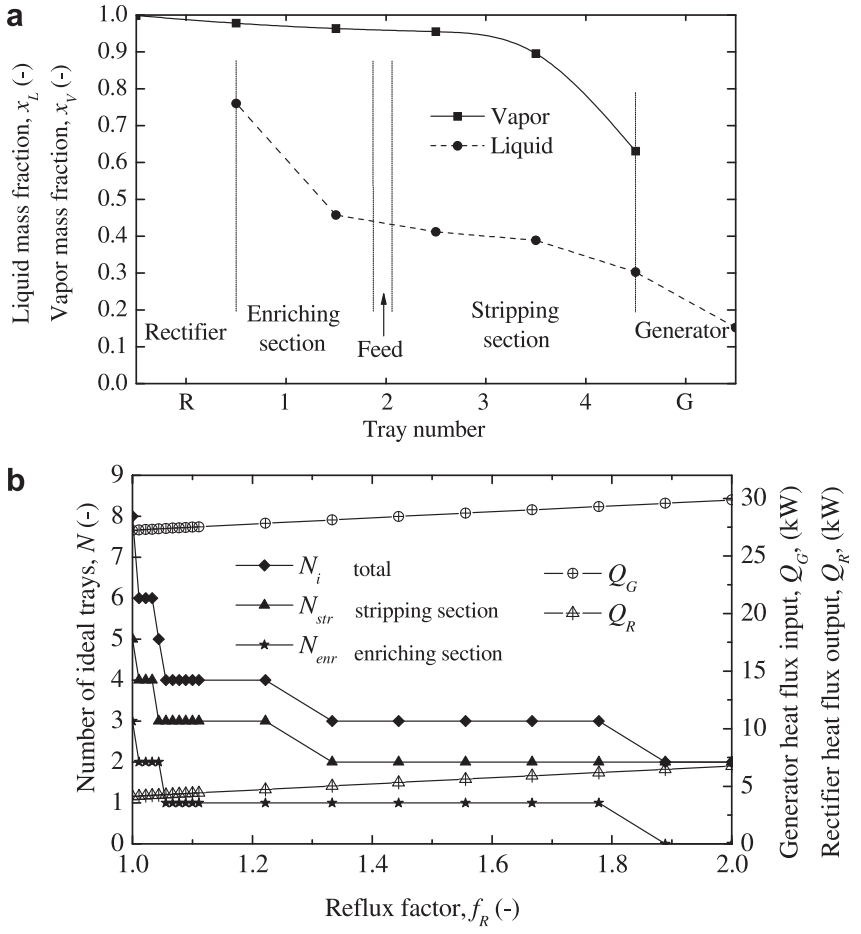

Fig. 4. (a) Vapor and liquid mass fraction variation in the column as a function of the reflux factor, (b) Number of trays and heat fluxes variation as a function of the reflux factor.

of ammonia vapor was found to be 4. Anand and Erickson [8] found that 6 was the ideal number of trays; Laouir et al. [18] obtained 3 ideal trays for a single-stage complete condensation *AARC* using a tridiagonal matrix method. Complete condensation leads to a lower *COP* [19] than just partial condensation. The number of the ideal trays depends basically on the reflux factor and the condensation type used. A sensitivity analysis of the number of trays is made below.

It can be seen in the Fig. 3b the input and exit heat flows in the distillation column, whose values were obtained from an energy and mass analysis for the control volumes CV-1, CV-2 and CV-3. The Ponchon-Savarit method also allowed the authors to calculate the heat flow to be delivered to the several parts of the distillation column. Heat flows to be supplied to the generator is $Q_G = 27.5$ kW, and since the cooling capacity of the cycle is $Q_E = 17.58$ kW (5 TR), the corresponding *COP* is 0.64. The heat flow that must be removed from the rectifier corresponds to $Q_R = 4.4$ kW. In Fig. 3c it can be noticed the temperature variation of the flow along the distillation column, vapor has its temperature decreased as it rises up and the liquid temperature increases as it descends, which is a typical behavior for countercurrent flows. The influx of strong solution to the column does not affect the column temperature profile since its temperature is close to temperatures for the liquid and vapor at entrance section. Changes of vapor and liquid mass fractions along the distillation column are shown in Fig. 4a. In that figure it can be observed the increase of the vapor mass fraction as it rises up in the column. The mass fraction variation in the stripping section is 51%, at the enriching section is 1.5%, and at the rectifier is 2.1%, these last two parts result in an ammonia vapor at a high grade of purity. Liquid mass flow decreases its concentration fast at the enriching section although in this section there exists only one tray, for other trays in the stripping section the variation is lower.

It can be shown that vapor mass flow increases upwards by 31% since it leaves the generator until reach the top of the first tray [14]. The increase in this flow is intensified at the point of the feeding section because of the large amount of ammonia. The variation of the liquid mass flow increases greatly in the second tray because of the feeding at the column. When the reflux ratio is equal to the minimum reflux ratio, the number of trays to suit the desired purification is the largest possible, as shown in graphs in Fig. 4b.

Table 2
Input variables to calculate the geometry of the column.

Variable	Value	
	Vapor	Liquid
Mass flow (kg/s)	0.0126	0.0400
Mass fraction (–)	0.6306	0.3025
Temperature (°C)	160.25	122.75
Ideal trays (–)	4	
Froth factor (–)	0.83	
Flooding factor (–)	0.80	
Weir length – column diameter ratio (–)	0.85	
Hole diameter (m)	0.003	
Tray thickness (m)	0.002	
Weir height (m)	0.01	

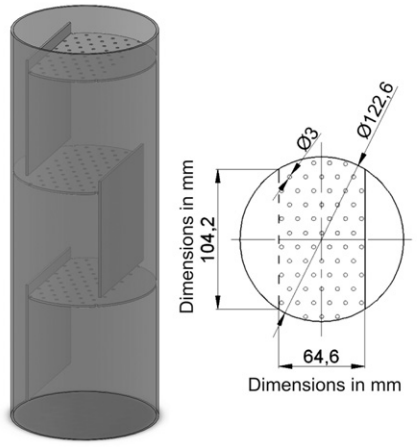

Variable	Value
Column diameter (m)	0.1226
Tray spacing (m)	0.1
Column height (m)	0.8
Actual tray number (-)	8
Weir length (m)	0.1042
Hole number (-)	61
Center hole tray pitch (m)	0.012
Column efficiency (%)	50
Vapor velocity after tray (m/s)	0.16
Hole vapor velocity (m/s)	3.64
Weepping vapor velocity (m/s)	2.22
Vapor pressure drop at tray (Pa)	265

Fig. 5. Geometry of the distillation column.

The graph shows that for this condition the number of ideal trays (N_i) required is 8. It can be seen that the number of trays is very sensitive when the reflux factor falls between 1 and 1.06. For higher reflux factors the number of trays becomes nearly constant. The stripping section will always have a larger number of trays (N_{str}) compared to the enrichment section (N_{enr}) one. For a reflux factor greater than 1.9 the trays in the enrichment section are no longer needed. Four ideal trays were selected in this work since because for a reflux factor between 1.06 and 1.22 the total number of ideal trays is exactly that figure. The heat flow that must be supplied to the generator is higher for higher reflux factors, since more liquid returns back to the column and, therefore, the *COP* will be also lower.

To calculate the main internal geometrical dimensions of the column, the column efficiency, and the actual number of trays, the necessary input variables are displayed in Table 2. The calculations were made for the bottom tray of the column.

Table 2 shows the values of mass flow rate, mass fraction, temperature, and ideal number of trays. The froth factor measures the ability of the system to generate foam. The flooding factor is the fraction of the flooding condition for which the column must operate [13]. Froth and flooding factors as well as the weir length-column diameter ratio shown in that table are typical values used in distillation columns [11,13,15]. Hole diameters between 1 mm and 25 mm are generally used in gas-liquid contact systems [16] such

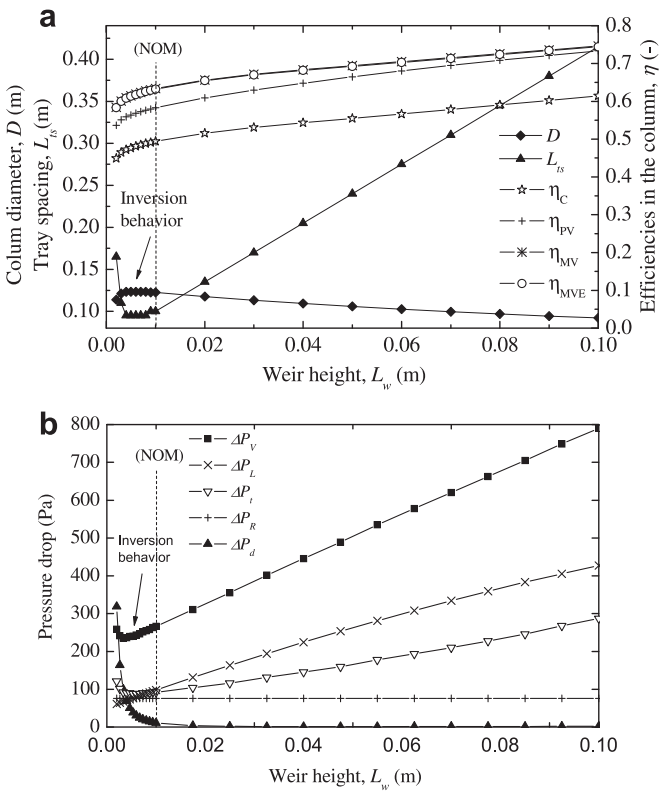

Fig. 6. (a) Size and column efficiency changes according to the weir height; (b) Pressure drop variation according to the weir height.

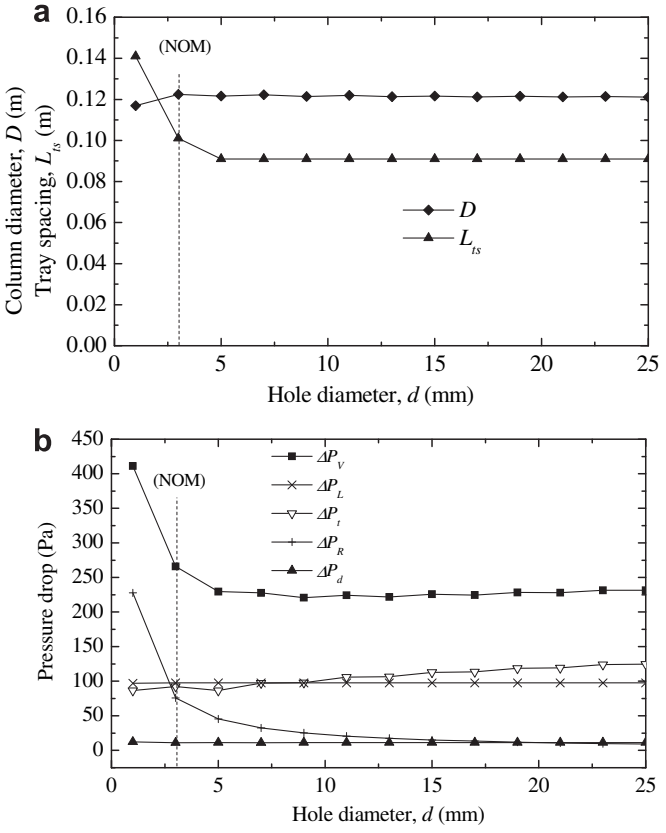

Fig. 7. Change in size (a) and the pressure drops (b) As a function of the hole diameter.

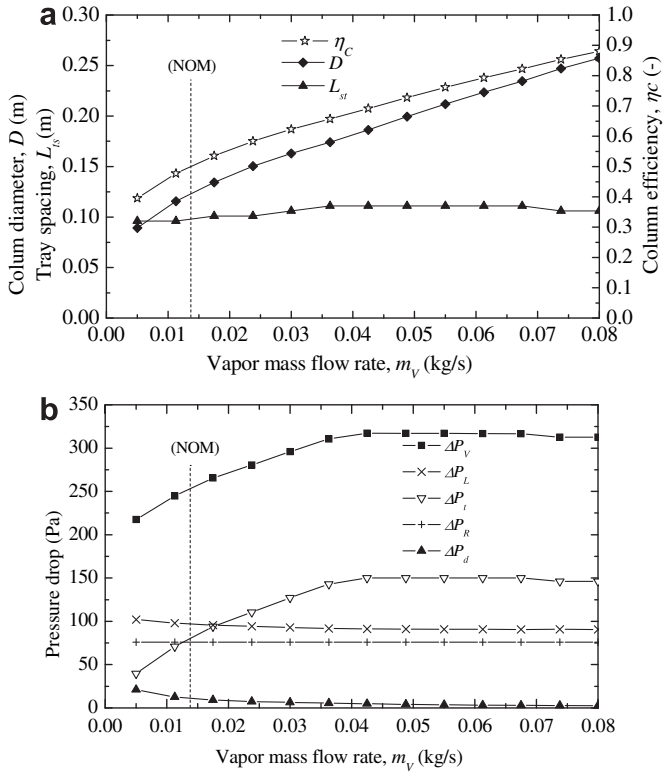

Fig. 8. (a) Size and column efficiency of the column variation as a function of the vapor mass flow, (b) Pressure drop variations as a function of the vapor mass flow rate.

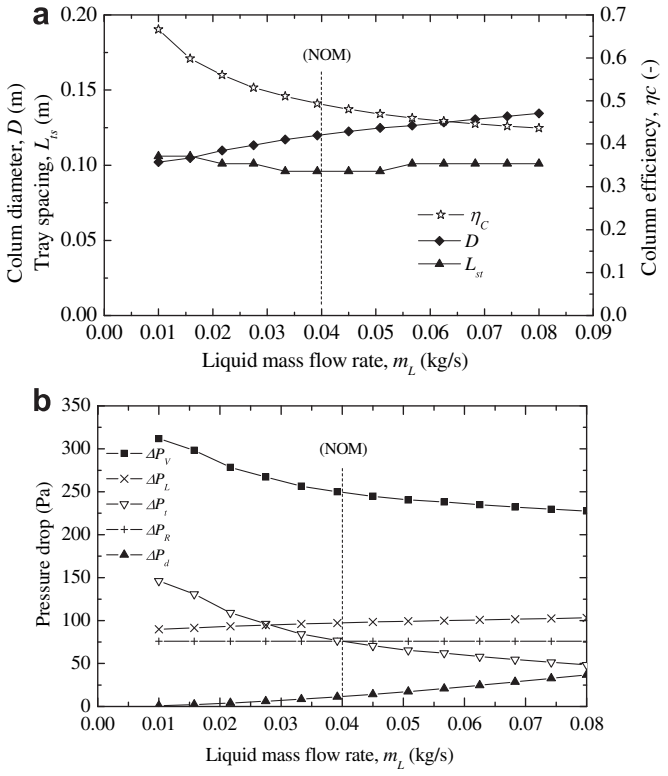

Fig. 9. (a) Size and column efficiency variation as a function of the liquid mass flow, (b) Pressure drop variation as a function of the liquid mass flow rate.

distillation columns, for a 3 mm hole diameter Treybal [11] recommends tray a thickness/hole diameter ratio of 0.65. It has been estimated a tray thickness of 2 mm. Weir height varies from 0 to 100 mm [13], an initial value of 10 mm was assumed. Holes pitch (usually in equilateral triangle shape) is 2.5–4 diameter hole [16] or 2.5 to 5 diameters [11]. In this work it was adopted 3.75 diameters.

Treybal [11] recommends that the tray spacing, L_{ts}, must be at least twice the level of liquid in the downcomer in order to avoid problems caused by entrainment of liquid in the downcomer. The results from the solution are summarized in Fig. 5.

The same calculation was carried out for the first tray, resulting in a column diameter of $D = 0.1204$ m. This represents a difference of 1.8% compared with the same calculation done for the last tray as seen in Fig. 5 ($D = 0.1226$ m). Kister [12] recommends that for differences greater than 20%, a good practice should be to use different column diameters. In the present case it was used the former one. The weeping vapor velocity [13] is smaller than the hole vapor velocity, so problems such as bypass is likely avoided.

It is carried out next a sensitivity analysis for the key geometrical variables that affect the overall column dimensions. Figs. 6–9 show the nominal (NOM) values of the variable in study in each case. Tray spacing is an indication of a column compactness design since if that distance is short, then the column height will also be short, which is a desirable feature in small absorption refrigeration appliances. As seen in graph of Fig. 6a the variable that greatly influences tray spacing L_{ts}, is the weir height, L_w. Tray spacing is a minimum for a weir height between 4 mm and 8 mm. For larger values of weir height, L_{ts} increases monotonically.

In Fig. 6a one can see that the column diameter reaches a maximum value for weir heights of around 6 mm. In Fig. 6b one can also see the variation of the following magnitudes: point efficiency (η_{PV}), Murphree (tray) efficiency (η_{MV}), Murphree corrected by entrainment efficiency (η_{MVE}), and column efficiency (η_c). The point efficiency is lower than the tray efficiency. One can notice that the entrainment does not influence appreciably the tray efficiency. The column efficiency results much less than that of Murphree's corrected by the entrainment efficiency; this is due to the fact that the column efficiency is strongly dependent of the liquid flow and when this is high compared to the vapor flow, the column efficiency decreases. By analyzing the graphs in Fig. 6a, one can conclude that a compact geometry can be achieved when the weir height is between 4 mm and 8 mm.

It can be seen in Fig. 6b that the vapor pressure drop (ΔP_v) increases with the weir height. It occurs because the vapor velocity (and so ΔP_t) and the liquid height (and so ΔP_L) increase. When the weir height is small, the passage area of the liquid under the downcomer is reduced, increasing the liquid velocity. It results an increasing in the liquid pressure drop when it flows through the downcomer (ΔP_d), however, when the weir height is higher, that pressure drop decreases.

Tray hole diameter (d), as shown in Fig. 7a, does not influence significantly the diameter of the column (D), but, the tray spacing (L_{ts}) becomes sensitive to hole diameters between 1 mm and 4 mm. Such a sensitivity is due to the fact that tray spacing is related to the amount of the liquid and vapor phases pressure drops. The latter increases because the residual pressure drop increases when hole diameters are smaller, as shown in Fig. 7b. It was found in this work that for hole diameter of 1 mm, the weeping vapor velocity [13] is very close to hole vapor velocity. To avoid bypass problems it is recommended that the hole diameter must be 2 mm or larger. Likewise, it is recommended to use hole diameters larger than 4 mm to achieve smaller pressure drops and tray spacing.

Considering the input variables in Table 2 and changing only the vapor flow, one can see its influence over the geometry of the column, as observed in Fig. 8a. It can be see that when the vapor

mass flow rate is increased, the diameter of the column tends also to increase. The column efficiency increases for higher vapor mass flow rates, as shown in Fig. 8a.

Tray spacing does not vary significantly with the vapor mass flow rate since the weir height is constant and the sum of pressure drops of the liquid and vapor remains almost constant, as can be seen in Fig. 8b. Dry pressure drop tray increases with the increasing of the vapor velocity. The weir height is constant, so the pressure drop of vapor passing through the liquid remains almost constant. The pressure drop of the liquid under the downcomer is slightly higher for lower vapor flow rates since the column diameter is smaller, as well as the passage area of the liquid under the downcomer.

When the liquid mass flow rate is increased, the required column diameter also increases, as shown in Fig. 9a. It occurs because the flooding velocity decreases with increasing the liquid flow, and to maintain the same volumetric flow of vapor, the diameter of the column must increase. The column efficiency decreases with increasing liquid flow mass flow rate, as shown in Fig. 9a, because the residence time of liquid on the tray decreases.

Since the weir height is nearly constant, the tray spacing depends only on the height of the liquid in the downcomer, which is connected to the sum of pressure drops of vapor and liquid, which remains almost constant as shown in Fig. 9b. Since the velocity of vapor decreases, the pressure drop in vapor to pass through the dry tray also decreases. The pressure drop of the liquid under the downcomer increases because of increased mass flow of liquid.

7. Conclusions

It was presented in this work an analysis of a distillation column with segmented weir sieve-tray of a 17.58 kW (5 TR) ammonia/water absorption refrigeration cycle. The Ponchon-Savarit method was used to carry out mass and energy balances in the distillation column as it is appropriate for solving distillation column problems. The calculation has shown that the stripping section provides a considerable increase in vapor concentration (51%), while the enrichment section increases the concentration of vapor only in 1.5% and the rectifier also in just 2.2%. The reflux factor happens to be an important economical parameter for designing a distillation column because the number of trays in the column and the required heat flow involved in the generator and rectifier are significantly dependent of it, mainly for values near to 1. The study allowed to calculate the internal geometry of the tray and the column. The tray spacing is sensitively to the weir height. The height of the column depends directly on the tray spacing, which is an indicating parameter of the compactness of the column. Weir height also influences directly the column diameter, column efficiency, and results have shown that optimal values fall between 4 mm and 8 mm, although for greater reliability it would to be used values greater than 8 mm. Column diameter is sensitive to the increasing of the vapor flow, and to a lesser extent to an increasing of the liquid flow. For hole diameters larger than 4 mm, the geometry of the column is insensitive, including pressure drop.

Acknowledgements

The authors thank FAPESP (project 2010/10858-4) for the project financial support. The first author also thanks FAPESP (2010/16304-0) for personal support and the second author thanks CNPq.

References

[1] J. Fernández-Seara, J. Sieres, Ammonia–water absorption refrigeration systems with flooded evaporators, Appl. Therm. Eng. 26 (2006) 2236–2246.
[2] J. Fernández-Seara, J. Sieres, The importance of the ammonia purification process in ammonia–water absorption systems, Energ. Convers. Manage. 47 (2006) 1975–1987.
[3] M. Ahachad, M. Charia, A. Bernatchou, A study of an improved NH_3-H_2O solar absorption refrigerating machine in Rabat (Morocco), Sol. Energ. Mat. Sol. C. 28 (1992) 71–79.
[4] K.E. Herold, R. Radermacher, S.A. Klein, Absorption Chillers and Heat Pumps, CRC Press, New York, 1996.
[5] M.J.P. Bogart, Pitfalls in ammonia absorption refrigeration, Int. J. Refrig. 5 (1982) 203–208.
[6] S.D. White, B.K. O'Neill, Analysis of an improved aqua-ammonia absorption refrigeration cycle employing evaporator blowdown to provide rectifier reflux, Appl. Energ. 50 (1995) 323–337.
[7] T.H. Kuehn, J.W. Ramsey, J.L. Threlkeld, Thermal Environmental Engineering, third ed. Prentice-Hall Upper Saddle River, New Jersey, 1998.
[8] G. Anand, D.C. Erickson, Compact sieve-tray distillation column for ammonia-water absorption heat pump: Part I – design methodology, ASHRAE Trans 105 (1999) 796–803.
[9] J. Sieres, J. Fernández-Seara, F. Uhía, Experimental characterization of the rectification process in ammonia–water absorption systems with a large-specific area corrugated sheet structured packing, Int. J. Refrig. 32 (2009) 1230–1240.
[10] G.A. Mendes, Study of vapor purification systems for a small absorption machine driven by solar energy (Estudo de sistemas de refinação de vapor numa máquina de absorção de pequena potência alimentada por energia solar. In Portuguese), Master Thesis, Universidade Técnica de Lisboa, Lisboa, Portugal, 2008.
[11] R.E. Treybal, Mass-Transfer Operations, third ed. McGraw-Hill Book Company, Singapore, 1981.
[12] H.D. Kister, Distillation Design, McGraw-Hill, USA, 1992.
[13] J.N. Caldas, A.I. Lacerda, E. Veloso, L.C.M. Paschoal, Tray and Packing Fillings in Columns. (Internos de Torres: Pratos e Recheios. In Portuguese), second ed. Interciência Ltda., Rio de Janeiro, 2007.
[14] E.W. Zavaleta-Aguilar, Thermal design of a distillation column of an ammonia/water absorption refrigeration cycle, (Modelagem térmica da coluna de destilação de um ciclo de refrigeração por absorção de amônia/água. In Portuguese), Master Thesis, São Paulo University, Brazil, 2010.
[15] M.J. Locket, Distillation Tray Fundamentals, Cambridge University, UK, 1986.
[16] R.H. Perry, D.H. Green, Perry's Chemical Engineers' Handbook, seventh ed. McGraw-Hill, USA, 1997.
[17] A.S.P. Ortigosa, F.C. Preter, R.L. Labozetto, E.W. Zavaleta-Aguilar, J.R. Simões-Moreira, Modeling, and simulation of a commercial ammonia – water absorption refrigeration cycle for production of chilled water, Proc. 13rd Brazilian Congress of Thermal Sciences and Engineering, Belo Horizonte, Brazil, 2008.
[18] A. Laouir, P. LeGoff, J.-M. Hornut, Cycles de frigopompes à absorption en cascades matérielles - détermination du nombre d'étages optimal pour le mélange ammonoiac-eau, Int. J. Refrig. 25 (2002) 136–148.
[19] J. Fernández-Seara, J. Sieres, M. Vázquez, Distillation column configurations in ammonia-water absorption refrigeration systems, Int. J. Refrig. 26 (2003) 28–34.